Appl Biochem Biotechnol (2014) 174:1201–1213
DOI 10.1007/s12010-014-1177-7

Thiol Modified Chitosan Self-Assembled Monolayer Platform for Nucleic Acid Biosensor

Maumita Das Mukherjee · Pratima R. Solanki · Gajjala Sumana · Takaaki Manaka · Mitsumasa Iwamoto · Bansi D. Malhotra

Received: 11 February 2014 / Accepted: 15 August 2014 /
Published online: 10 September 2014

Abstract A self-assembled monolayer (SAM) of thiol modified chitosan (SH-CHIT), with thioglycolic acid (TGA) as a modifier to bestow thiol groups, has been prepared onto gold (Au)-coated glass plates for fabrication of the nucleic acid biosensor. The chemical modification of CHIT via TGA has been evidenced by Fourier transform infrared spectroscopy (FT-IR) studies, and the biocompatibility studies reveal that CHIT retains its biocompatible nature after chemical modification. The electrochemical studies conducted onto SH-CHIT/Au electrode reveal that thiol modification in CHIT amino end enhances the electrochemical behavior indicating that it may be attributed to delocalization of electrons in CHIT skeleton that participates in the resonance process. The carboxyl group modified end of DNA probe has been immobilized onto SH-CHIT/Au electrode using *N*-ethyl-*N*′-(3-dimethylaminopropyl) carbodimide (EDC) and *N*-hydroxysuccinimide (NHS) chemistry for detection of complementary, one-base mismatch and non-complementary sequence using electrochemical and optical studies for *Mycobacterium tuberculosis* detection. It has been found that DNA-SH-CHIT/Au bioelectrode can specifically detect 0.01 μM of target DNA concentration with sensitivity of 1.69×10^{-6} A μM^{-1}.

M. D. Mukherjee
Amity Institute of Applied Sciences, Amity University, Noida, Uttar Pradesh, India

P. R. Solanki
Special Centre for Nanoscience, Jawaharlal Nehru University, New Delhi, India

G. Sumana · B. D. Malhotra
Department of Science and Technology Centre on Biomolecular Electronics, Biomedical Instrumentation Section, Materials Physics and Engineering Division, CSIR- National Physical Laboratory, New Delhi 110012, India

T. Manaka · M. Iwamoto
Department of Physical Electronics, Tokyo Institute of Technology, 2-12-1 O-okayama Meguro-ku, Tokyo 152-8552, Japan

B. D. Malhotra (✉)
Department of Biotechnology, Delhi Technological University, Main Bawana Road, Shahbad Daulatpur, Delhi 110042, India
e-mail: bansi.malhotra@gmail.com

Keywords Thiol modified chitosan · DNA biosensor · Surface plasmon resonance · *Mycobacterium tuberculosis*

Introduction

In recent years, there is an increased interest towards the development of nucleic acid biosensors for clinical monitoring of the infectious diseases, especially those resulting from life-threatening pathogens. In addition to the clinical monitoring, the change in the DNA redox properties (oxidation of guanine), redox indicator-based indirect electrochemistry, considered to be an important alternative for development of nucleic acid hybridization biosensors which offer advantages in terms of reusability and sensitivity. Besides this, electrochemical biosensors do not require additional labeling step and can be easily integrated with electronics for fabrication of miniaturized devices for diagnosis of infectious diseases and the detection of pathogenic biological species of environmental and clinical interests [1, 2].

Tuberculosis is presently the chronic pulmonary bacterial infectious disease, caused by *Mycobacterium tuberculosis*. According to the World Health Organization (WHO), nearly two billion people in the present world's population have been exposed to the tuberculosis pathogen. It is the world's greatest infectious killer of women of reproductive age and is the leading cause of death among people with HIV/AIDS [3, 4]. The resurgence of TB and increased risk for TB in HIV-infected persons has intensified the requirement for a rapid, cost-effective method for diagnosis. Conventional diagnostic methods such as polymerase chain reaction (PCR) and restriction fragment length polymorphism (RFLP) are time consuming and require trained expertise. There is, thus, an urgent need for sensitive, specific, stable, cost-effective, and reusable method for *M. tuberculosis* detection. In this context, affinity biosensors have emerged as promising alternative for microbial detection using nucleic-acid-based detection of complementary target sequences [5–8].

Lately, there is an enhanced interest to minimize denaturation of biomolecules and to achieve rapid electron transfer at desired surfaces. Among the various strategies used for modification of the electrode surfaces, self-assembled monolayer (SAM) exhibit unprecedented flexibility to tailor interfacial properties and present biologically relevant groups. The SAMs are considered to be more suitable for biosensing, since they are easy to form and have increased stability, reusability, ordered arrangement, and high reproducibility. SAMs of functionalized silanes, alkanes, or polymers have been found to be useful for anchoring proteins, enzymes, and DNA for fabrication of biosensors as these may provide the interface between the transducer and the analyte for faster signal detection [9–11].

Chitosan (CHIT) and its derivatives have been found to be suitable for immobilization of desired biomolecules because of the excellent film-forming ability, high permeability, mechanical strength, biocompatibility, and low cost. Moreover, chemical modification of the amino groups of CHIT provides hydrophilic environment for biomolecules. Recently, CHIT and their composites deposited using sol-gel technique; spin coating and electrochemical deposition have successfully been applied for the development of biosensors [12]. However, using these techniques, the constant thickness, and uniformity is very difficult to achieve resulting in complexity in getting the reproducibility.

In this manuscript, we report the thiolation of chitosan (SH-CHIT) at amino ($-NH_2$) ends, with thioglycolic acid (TGA) via amide bond formation, and its self-assembled monolayer has been fabricated on gold (Au) surface using Au-SH affinity interaction. The SH-CHIT/Au electrode has been utilized for the fabrication of DNA biosensor for *M. tuberculosis* using

surface plasmon resonance (SPR) technique utilizing the advantage of CHIT-SAM onto Au surface. Besides this, electrochemical transducer has been used to detect the hybridization event as SH-CHIT/Au electrode shows improved electrochemical properties compared to CHIT/Au, which may be attributed to the conjugation of electrons in SH-CHIT skeleton [13–15].

Materials and Method

Low molecular weight chitosan (Mw 2.4×10^6), *N*-ethyl-*N*′-(3-dimethylaminopropyl) carbodimide (EDC), *N*-hydroxysuccinimide (NHS), thioglycolic acid (TGA), oligonucleotide probe sequence specific to *M. tuberculosis*, complementary target, one-base mismatch, and non-complementary DNA sequences have been purchased from Sigma-Aldrich, USA. All the solutions and glassware are autoclaved prior to being used, and desired reagents (molecular biology grade) have been prepared in de-ionized water (Milli Q 10 TS). The 50-nm-thick Au-coated BK-7 glass plates (24 mm diameter) are procured from Autolab, The Netherlands. Pre-cleaned (with piranha solution, H_2SO_4: H_2O_2=7:3, for about 5 min followed by rinsing in de-ionized water) Au-coated glass plates have been used as substrates for deposition of thiolated chitosan SAM. The sequence of DNA probes used for the DNA hybridization detection is as follows:

Probe : Carboxyl-GAA-CAA-CCC-GCT-GTC-GGG-GT

Complementary : AC-CCC-GAC-AGC-GGG-TTG-TTC

One-base mismatch : AC-CCC-GTC-AGC-GGG-TTG-TTC

Non-complementary : CG-GCG-CAG-TGG-ATA-GCT-GCA

Fabrication of the Thiol Modified Chitosan Film onto Au Electrode

For the fabrication of SH-CHIT SAM, Au-coated BK-7 glass plates have been immersed in 0.1 M TGA in water, along with 50 mM EDC, 1.0 g of CHIT, and 4 mL of acetic acid, and kept overnight at room temperature [16, 17]. TGA is reacted with CHIT in dilute solution for covalent binding of the acids with amine groups of CHIT, resulting in amide bond formation. CHIT is reacted in the presence of a carbodiimide to facilitate amide-forming condensation reaction. For each synthetic reaction, pH is adjusted to 4.5–5.0. After the coupling reaction, electrodes are rinsed with water to remove physically adsorbed SH-CHIT from the Au surface and then dried under a stream of nitrogen.

Immobilization of ssDNA Probe on SH-CHIT/Au Electrode and Hybridization with Complementary Target Analyte

Carboxyl (−COOH) functionalized 20-mer probe DNA (ssDNA) is immobilized onto SH-CHIT/Au surface using EDC-NHS carbodiimide chemistry (DNA-SH-CHIT/Au). One milliliter of 100 μM of −COOH-ssDNA is activated with EDC (100 mM) in presence of 200 mM NHS for about 24 h at room temperature (25 °C). This activated DNA is covalently immobilized onto SH-CHIT/Au surface using −OH functionality of CHIT via ester bond formation between −COOH of DNA and −OH of CHIT (Scheme 1). The electrode is rinsed

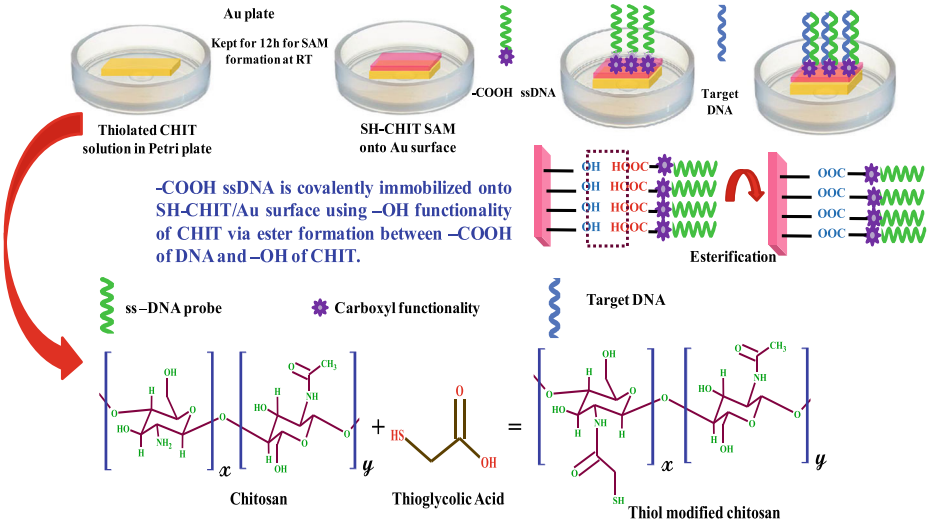

Scheme 1 Chemical modification of CHIT with TGA, fabrication of SH-CHIT SAM onto Au surface using SH-Au affinity interaction and immobilization of carboxyl functionalized DNA onto SH-CHIT/Au surface

three times with phosphate buffer (pH 7.0) to remove any unimmobilized ssDNA. The hybridization is performed at 25 °C by incubating DNA-SH-CHIT/Au bioelectrode with complementary target and non-complementary and one-base mismatch DNA sequences of different concentration for about 60 s. The electrode is washed with phosphate buffer (pH 7.0) to remove any unhybridized DNA.

For the hybridization studies, a stock solution of 100 μM of target DNA has been prepared and dilution is made in buffer solution up to the desired concentration i.e. 0.01 μM. Five microliters of the target DNA solution was added to DNA-SH-CHIT/Au electrode, and their electrochemical response was studied by differential pulse voltammetry (DPV) technique in PBS (50 mM, pH 7.0, 0.9 % NaCl) using methylene blue (MB) as redox indicator.

Characterization

CHIT/Au, SH-CHIT/Au, and DNA-SH-CHIT/Au electrodes have been characterized by Fourier transform infrared spectroscopy (FT-IR, PerkinElmer, Spectrum BX II), contact angle measurements (CA-Dataphysics, Germany, model: OCA 15EL), and high-resolution transmission electron microscopy (HR-TEM, Tecnai-G2 F30 STWIN with field emission gun electron source) studies. Electrochemical analysis has been conducted using Autolab Potentiostat/Galvanostat (Eco Chemie, AD Utrecht, The Netherlands) using a three-electrode system with Au as working electrode, platinum wire as auxiliary electrode, and Ag/AgCl as reference electrode in PBS (50 mM, pH 7.0) containing 5 mM $[Fe(CN)_6]^{3-/4-}$ as redox probe. The hybridization experiments using SPR have been carried out using an Autolab SPR, Eco Chemie (Netherlands), based on the traditional Kretschmann configuration. In SPR experiments, linearly *p*-polarized light from a laser (670 nm) is directed to a prism onto the gold electrode, and the intensity of reflected light is measured over a range of 4,000 millidegrees (m°) at 25 °C as a function of time. An index matching fluid (SPR oil) has been used for coupling the gold-coated glass electrode with the plane. In this experiment, a gold-coated glass electrode is coupled with the plane face of the prism.

Results and Discussion

Fourier Transformed Infrared Studies

The chemical modification of CHIT with TGA has been confirmed by FT-IR studies (film thickness 100 nm) and is depicted in Fig. 1a. Evidence of conversion of the amine group of CHIT is seen from the observed decrease of the amine N-H bend signal at 1,596 cm^{-1} in SH-CHIT. Coupled with the loss of amine signal indicates the formation of amide in SH-CHIT, with the appearance of amide I and amide II band signals at 1,657 and 1,562 cm^{-1}, respectively. It can be seen that the C-O-C stretch near 1,100 cm^{-1} remains essentially unchanged in SH-CHIT/Au and CHIT/Au electrodes [18].

Scanning Electron and Transmission Electron Microscopic Studies

The scanning electron microscopic (SEM) analysis of SH-CHIT/Au electrode shows uniform and rough surface morphology (Fig. 1b) indicating the homogeneous SAM formation onto Au surface. The transmission electron microscopic (TEM) images of SH-CHIT/Au electrode (Fig. 1b) show featureless grains with individual grain size of 1–2 μm. The corresponding EDX clearly reveals the presence of elements like carbon, nitrogen, oxygen, phosphorous, and sulfur. The existence of sulfur is attributed to the thiolation of the CHIT polymeric chain as also confirmed by FT-IR data.

Contact Angle Measurement

Contact angle (CA) technique based on sessile drop method has been used to explain the hydrophilic/hydrophobic nature of the surface as the quality of the monolayer can be estimated from the wetting measurement; the shape of the liquid drop is affected by the free energy of the surface. Figure 2a shows CA studies of blank Au (i), SH-CHIT/Au (ii), and DNA-SH-CHIT/Au (iii) electrodes, respectively. The change in CA value indicates the modification of CHIT film onto bare Au surface and immobilization of ssDNA onto SH-CHIT/Au film [19]. The CA value obtained as 64° for blank Au surface reveals both clean as well as hydrophobic nature of the surface. The value decreases to 50° after SH-CHIT SAM formation which may be attributed to the hydrophilic nature of CHIT due to presence of the OH groups. Further, the CA value decreases to 32° after DNA immobilization revealing the presence of hydrophilic phosphate backbone of DNA bound onto the SH-CHIT/Au electrode.

Biocompatibility Studies Using Bacterial and Plant Systems

The biocompatibility of SH-CHIT solution of 0.1 mg mL^{-1} concentration has been investigated with both the bacterial and plant systems. For the bacterial system (Fig. 2b), a culture is grown overnight in a nutrient broth medium at 30 °C in a rotary shaker at 150 rpm. One hundred microliters of the culture is spread on a nutrient agar plate, and wells (2 mm diameter) are made with the sterile core borer. Ten microliters of the SH-CHIT solution is added to the wells and kept for incubation at 30 °C. After ~48 h of incubation, no zone of inhibition is seen in the plate, indicating biosafety of the compound. For plant germination (Fig. 2c), wheat (i) and mustard (ii) seeds are immersed in solution of SH-CHIT solution and placed on soft agar for germination. After incubation at 30 °C in the dark for 4 days (for wheat seeds) and 7 days (for mustard seeds), germination is checked and compared with that of the controlled seeds. The observations pertaining to the effect of SH-CHIT solution on seed germination reveal

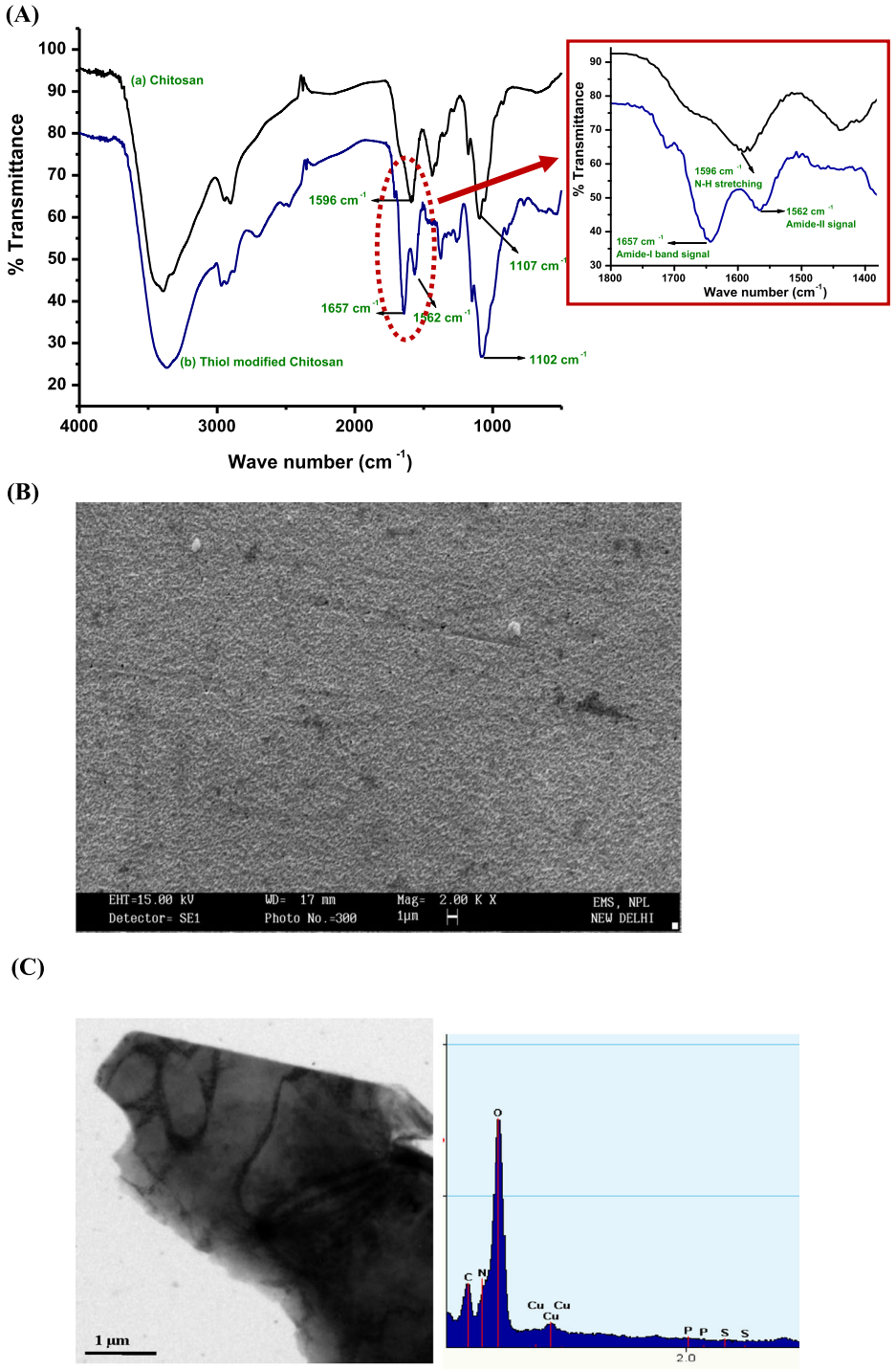

Fig. 1 **a** FT-IR spectra of *a* CHIT onto gold surface and *b* thiol modified CHIT onto gold surface. **b** SEM image of SH-CHIT/Au surface. **c** TEM and corresponding EDX of SH-CHIT solution

appropriate seed germination in wheat and mustard seeds, indicating once again the biocompatible nature of this nanocomposite.

Electrochemical Studies

Figure 3a shows results of cyclic voltammetric (CV) studies of (i) SH-CHIT/Au, (ii) CHIT/Au, and (iii) DNA-SH-CHIT/Au electrodes in PBS (50 mM, pH 7.0, 0.9 % NaCl) containing

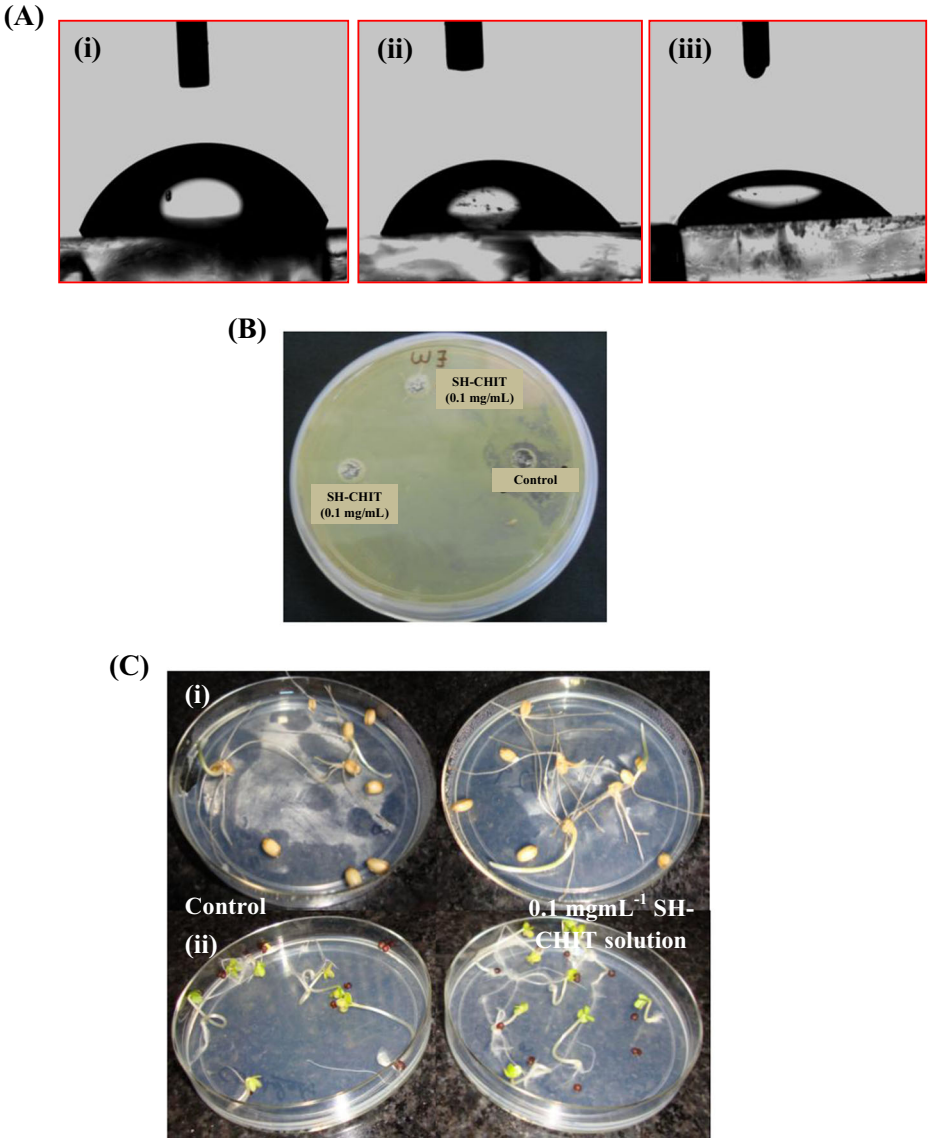

Fig. 2 **a** Contact angle of *i* blank Au, *ii* S-CH/Au, and *iii* DNA-S-CH/Au bioelectrodes; Snapshot of the agar plates containing **b** *Pseudomonas* sp. after 48 h of incubation, revealing no inhibition zone formation in the plate using SH-CHIT solution and **c** wheat (*i*) and mustard (*ii*) seeds after 4 and 7 days of incubation, respectively, revealing proper seed germination, showing the biocompatibility of SH-CHIT solution even after thiolation

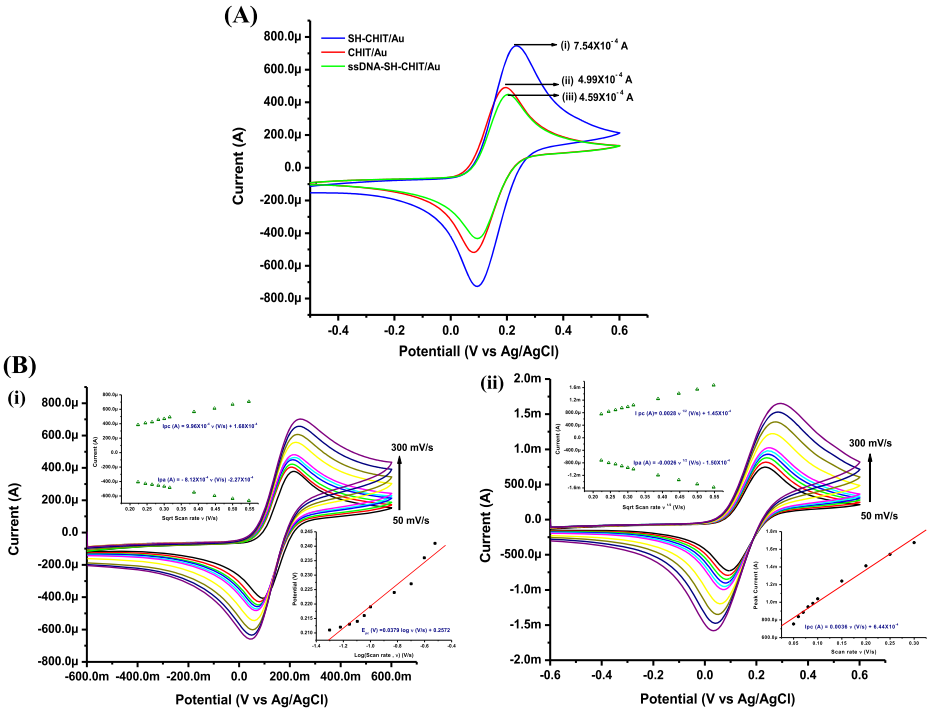

Fig. 3 Cyclic voltammetric studies of **a** SH-CHIT/Au (*i*), CHIT/Au (*ii*), and DNA-SH-CHIT/Au (*iii*) electrodes. **b** CHIT/Au (*i*) and SH-CHIT/Au (*ii*) electrodes as a function of scan rate (50–300 mV/s) in PBS (50 mM, pH 7.0, 0.9 % NaCl) containing 5 mM $[Fe(CN)_6]^{3-/4-}$ (*inset* plot of peak current vs. $\nu^{1/2}$ (V/s) and peak potential vs. scan rate ν (V)) in PBS (50 mM, pH 7.0, 0.9 % NaCl) containing 5 mM $[Fe(CN)_6]^{3-/4-}$

5 mM $[Fe(CN)_6]^{3-/4-}$ in the potential range of −0.6 to 0.7 V at a scan rate of 50 mV/s. CV of CHIT/Au shows a well-defined redox behavior (curve ii) at 0.197 V (E_{pc}), and the anodic peak potential (E_{pa}) at 0.082 V with cathodic peak current of 4.99×10^{-4} A. This may be due to cationic CHIT that accepts electrons from ferricyanide species resulting in enhanced redox current. The magnitude of current response for SH-CHIT/Au electrode (curve i) increases (7.54×10^{-4} A) in comparison to that of CHIT/Au electrode. This may be due to the fact that after thiolation, two pairs of electrons are in conjugation with CHIT skeleton and participate in resonance which is absent in pristine CHIT with one lone pair fixed onto $-NH_2$ group. Moreover, peak-to-peak separation of 0.13 V for SH-CHIT/Au electrode suggests that the redox behavior approaches towards perfectly reversible system. After immobilization of ssDNA onto SH-CHIT/Au surface, the peak current value decreases to 4.59×10^{-4} A, which may be attributed to repulsion between negatively charged DNA and $[Fe(CN)_6]^{3-/4-}$ moieties present in PBS, resulting in inhibited electron transfer kinetics. CVs of both CHIT/Au and SH-CHIT/Au electrodes as a function of scan rate (50–300 mV/s) in PBS (50 mM, pH 7.0, 0.9 % NaCl) containing 5 mM $[Fe(CN)_6]^{3-/4-}$ have been studied to estimate number of ionic species per unit area (Γ) and found that 0.27×10^{-8} and 0.765×10^{-8} mol.cm^{-2}, respectively (Fig. 3b). The higher Γ for SH-CHIT/Au electrode indicates that large number of redox moieties are available for oxidation leading to higher faradic current wherein, the presence of delocalized electrons due to thiolation, results in increased electron transport between redox species and electrode [20–24].

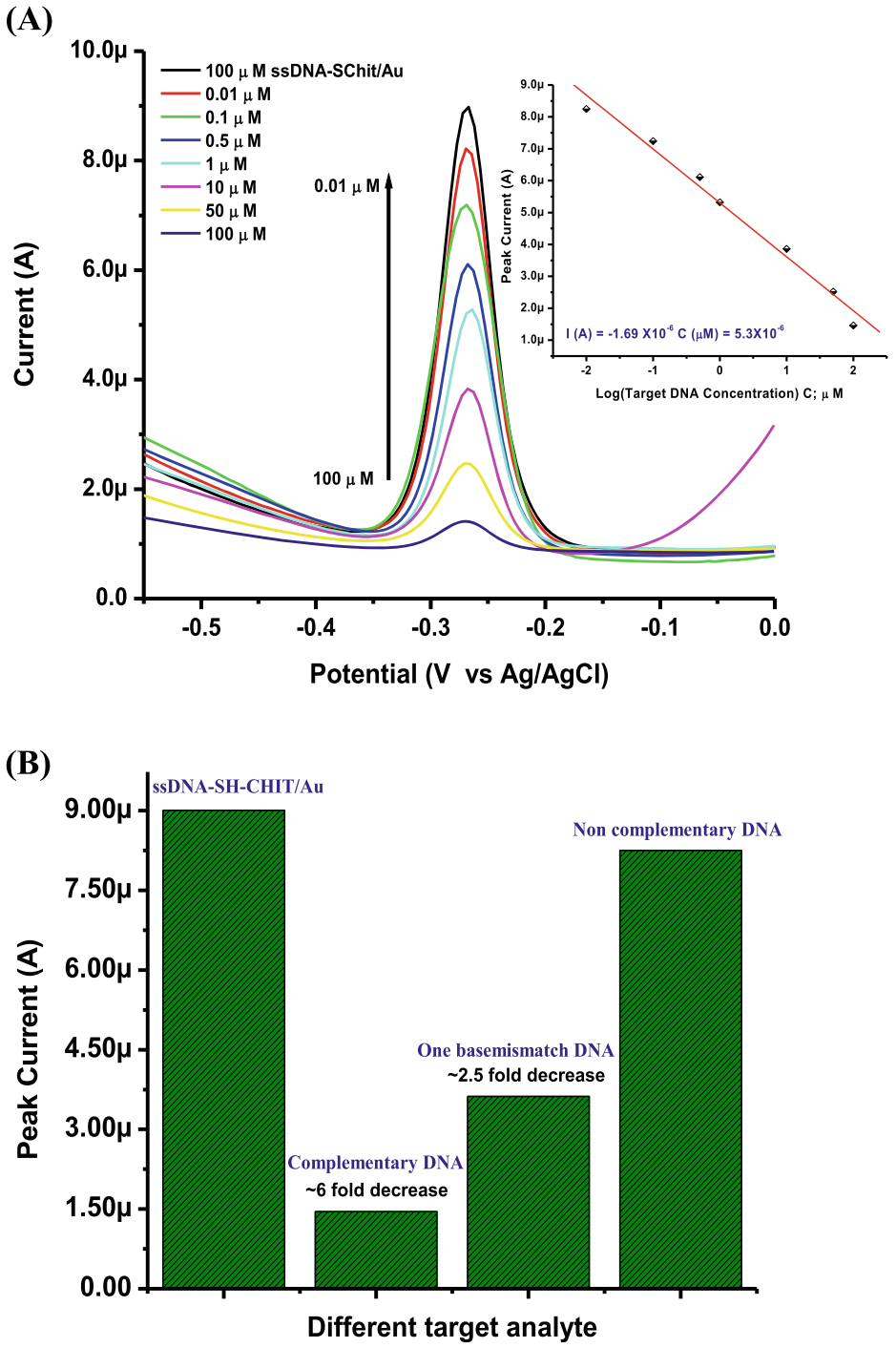

Fig. 4 **a** DPV response of ssDNA-SH-CHIT/Au bioelectrode after hybridization with complementary target DNA in PBS containing MB as indicator. **b** Bar diagram of selectivity studies of ssDNA-SH-CHIT/Au, with complementary, one-base mismatch and non-complementary target DNA of 100 μM concentration

Electrochemical Response Studies

The electrochemical response of ssDNA-SH-CHIT/Au bioelectrode after hybridization with 0.01–100 μM of complementary target DNA (dsDNA) has been studied by differential pulse voltammetry (DPV) technique in PBS (50 mM, pH 7.0, 0.9 % NaCl) using methylene blue (MB) as redox indicator. The magnitude of current with respect to MB changes after hybridization of probe with target (Fig. 4a). It has been observed that magnitude of current response decreases with increased complementary DNA concentration (inset, Fig. 3b). This may be due to enhanced number of target DNA molecules onto ssDNA-SH-CHIT/Au

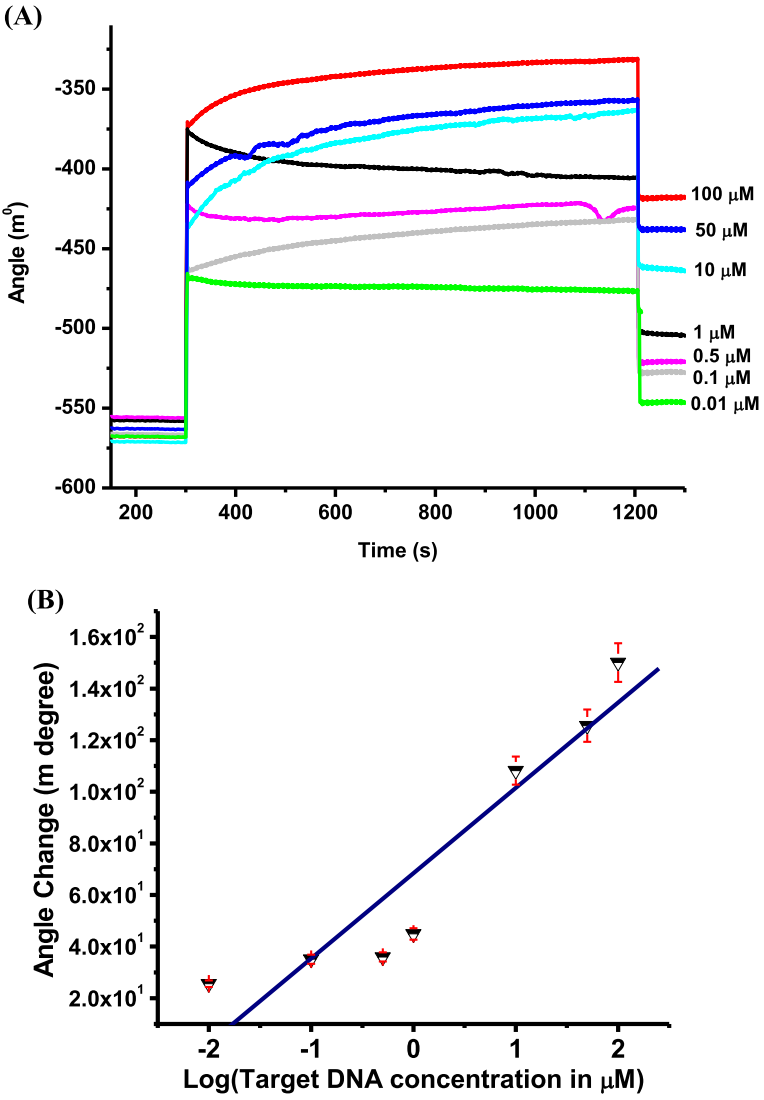

Fig. 5 **a** SPR sensorgrams for covalent immobilization of ssDNA onto SH-CHIT/Au. **b** Linearity curve of target DNA concentration in micromolar against angle in SPR angle in millidegrees

bioelectrode resulting in steric inhibition of MB packing between double helix of the hybrid. It has been observed that decrease in the MB peak with respect to target concentration follows Eq. 1.

$$\mathrm{I(A)\ dsDNA} = -1.69 \times 10^{-6} \times \log\left[\text{DNA concentration in } \mu\mathrm{M}\right] + 5.3 \times 10^{-6} \quad (1)$$

The detection limit of ssDNA-SH-CHIT/Au bioelectrode is 0.01 μM with sensitivity of 1.69×10^{-6} A μM^{-1}.

The selectivity of ssDNA-SH-CHIT/Au bioelectrode has been investigated by examining the interaction of ssDNA-SH-CHIT/Au bioelectrode (Fig. 4b) with the complementary, one-base mismatch and non-complementary DNA sequence. When ssDNA-SH-CHIT/Au bioelectrode is incubated with non-complementary target DNA, negligible change in the signal is observed reflecting the expected absence of hybridization. However, after incubation with the complementary target analyte and one-base mismatched sequence, the magnitude of MB signal decreases down to ~sixfold and ~2.5-fold, respectively. The results demonstrate that only complementary target DNA hybridizes with the probe DNA (ssDNA) leading to significant decrease in the DPV signal. The observed negligible change in the signal observed for the non-complementary sequence shows high selectivity of the hybridization detection [25–27].

Surface Plasmon Resonance Studies

The DNA probe solutions (100 μM) are immobilized onto the SH-CHIT/Au surface and used for hybridization studies with the complementary DNA sequences using SPR technique. During SPR measurements, the baseline is corrected for about 300 s using the autoclaved de-ionized water to remove any unbound DNA molecules. After the baseline correction, complementary DNA sequences are allowed for the association phase for about 900 s. On completion of the association phase, the unbound solution is discarded and the electrode is washed with de-ionized water (dissociation phase; 200 s). The change in the SPR angle before and after the association phase corresponding to the amount of DNA hybridized has been monitored, while keeping all other parameters constant. After completion of the dissociation phase, the surface is fully regenerated by washing with HCl solution (5.0 mM) for 120 s (data not shown).

Figure 5a shows results of SPR studies of ssDNA-SH-CHIT/Au bioelectrode for detection of hybridization with the complementary target DNA having concentration from 0.01 to 100 μM. It is observed that change in the SPR angle decreases with decrease in the complementary DNA concentration, resulting in lesser availability of the complementary

Table 1 Various biosensing parameters of SH-CHIT/Au electrode in comparison with those based on other CHIT-based nanocomposites

Matrix	Analyte	Transducer used	Detection limit	Reference
Covalently cross-linked chitosan	Catechol	Amperometric	10 nM	29
Chitosan/layered double hydroxides organic-inorganic composite	Catechol	Amperometric	0.36 nM	30
Chitosan/tetrakis(2-hydroxyethyl) orthosilicates composite	H_2O_2	Amperometric	4×10^{-7} mol/L	31
Chitosan-coupled carbon nanotubes on polyaniline-modified gold electrode	GOD	Amperometric	0.1 mM	32
Thiol modified chitosan	DNA	SPR and electrochemical	0.01 μM	Present work

DNA towards probe or presence of less mass loading onto the surface. The change in SPR signal of ssDNA-SH-CHIT/Au bioelectrode has been measured from 25.64 to 150.00 m° after hybridization with the complementary target (100 μM) indicating complete saturation of the electrode. The change in the SPR angle varies linearly with increased concentration (Fig. 5b). The control experiment using de-ionized water has been conducted, and no significant change in SPR angle is observed (data not shown). Table 1 shows the various biosensing parameters of SH-CHIT/Au electrode in comparison with those reported in the literature based on other CHIT-based nanocomposites

Conclusions

Thiol modified CHIT by TGA has been used to fabricate SAM onto Au surface using SH-Au affinity interaction which in turn helps to capture the DNA hybridization event using SPR. FT-IR studies confirm thiol incorporation into the CHIT skeleton, and biocompatibility studies indicate that the biocompatible nature of CHIT remains intact after thiol modification. Cyclic voltammetric studies have revealed that these SH-CHIT/Au electrode exhibits enhanced electrochemical properties due to the delocalized electrons that participate in resonance. The ssDNA-SH-CHIT/Au bioelectrode exhibits high sensitivity (1.69×10^{-6}A μM^{-1}) towards hybridization detection (0.01–100 μM complementary DNA) using DPV and SPR technique. SH-CHIT/Au platform can be used for fabrication of other electrochemical DNA biosensor for the detection of clinically important analyte such as cholera, *Neisseria gonorrhoeae*, etc.

Acknowledgments We thank Prof. R.C. Budhani, Director, National Physical Laboratory, India for the facilities. Maumita Das Mukherjee is thankful to Amity University, Noida for allowing her to perform the experiments. The financial support received at NPL, from Department of Science and Technology, India under the projects GAP 081132 and GAP 080232 is greatly acknowledged.

References

1. Leegsma-Vogt, G., Rhemrev-Boom, M. M., Tiessen, R. G., Venema, K., Korf, J., Jeffrey, M., Halliday, W. G., & Taylor, K. C. (2004). *Biomedical Materials and Engineering, 14*, 455–464.
2. Singh, R., Verma, R., Sumana, G., Srivastava, A. K., Sood, S., Gupta, R. K., & Malhotra, B. D. (2012). *Bioelectrochemistry, 86*, 30–37.
3. Das, M., Sumana, G., Nagarajan, R., & Malhotra, B. D. (2010). *Applied Physics Letters, 96*, 133706.
4. Das, M., Dhand, C., Sumana, G., Srivasrava, A. K., Nagarajan, R., Nain, L., Iwamoto, M., Manaka, T., & Malhotra, B. D. (2011). *Biomacromolecules, 12*, 540–547.
5. Chun, A. L. (2009). *Nature Nanotechnology, 4*, 698–699.
6. Thanyani, S. T., Robert, V., Siko, D. R. G., Very, P., & Verschoor, J. A. (2008). *Journal of Immunological Methods, 332*, 61–72.
7. Russell, D. G. (2001). *Nature Reviews Molecular Cell Biology, 2*, 569–577.
8. Good, M. C., Greenstein, A. E., Young, T. A., Ng, H. L., & Albert, T. (2004). *Journal of Molecular Biology, 339*, 459–469.
9. Wang, L., & Wang, E. (2004). *Electrochemistry Communications, 6*, 49–54.
10. Shan, D., Han, E., Xue, H., & Cosnier, S. (2007). *Biomacromolecules, 8*, 3041–3046.
11. Francia, G. D., Ferrara, V. L., Manzo, S., & Chiavarini, S. (2005). *Biosensors and Bioelectronics, 21*, 661–665.

12. Kaushik, A., Solanki, P. R., Ansari, A. A., Ahmad, S., & Malhotra, B. D. (2008). *Electrochemistry Communications, 10*, 1364–1368.
13. Guggi, D., Langoth, N., Hoffer, M. H., Wirth, M., & Schnurch, A. B. (2004). *Journal of Pharmacognosy, 278*, 353–360.
14. Solanki, P. R., Arya, S. K., Nishimura, Y., Iwamoto, M., & Malhotra, B. D. (2007). *Langmuir, 23*, 7398–7403.
15. Solanki, P. R., Prabhakar, N., Pandey, M. K., & Malhotra, B. D. (2008). *Biomedical Microdevices, 10*, 757–767.
16. Zhu, X., Su, M., Tang, S., Wang, L., Liang, X., Meng, F., Hong, Y., & Xu, Z. (2012). *Molecular Vision, 18*, 1973–1982.
17. Schnürch, A. B., Hornof, M., & Zoidl, T. (2003). *International Journal of Pharmaceutics, 260*, 229–237.
18. Cathell, M. D., Szewczyk, J. C., Bui, F. A., Weber, C. A., Wolever, J. D., Kang, J., & Schauer, C. L. (2008). *Biomacromolecules, 9*, 289–295.
19. Arya, S. K., Prusty, A. K., Singh, S. P., Solanki, P. R., Pandey, M. K., Datta, M., & Malhotra, B. D. (2007). *Analytical Biochemistry, 363*, 210–218.
20. Singh, A., Sinsinbar, G., Choudhary, M., Kumar, V., Pasricha, R., Verma, H. N., Singh, S. P., & Arora, K. (2013). *Sensors and Actuators B: Chemical, 185*, 675–684.
21. Zhao, G., Xu, J., & Chen, H. (2006). *Electrochemistry Communications, 8*, 148–154.
22. Yang, M., Yang, Y., Yang, H., Shen, G., & Yu, R. (2006). *Biomaterials, 27*, 246–255.
23. Zhuang, Q., Hen, J., Chen, J., & Lin, X. (2008). *Sensors and Actuators B: Chemical, 128*, 500–506.
24. Hu, G., Zhang, D., Wu, W., & Yang, Z. (2008). *Colloids and Surfaces B: Biointerfaces, 62*, 199–205.
25. Liao, J. C., Mastali, M., Li, Y., Gau, V., Suchard, M. A., Babbitt, J., Gornbein, J., Landaw, E. M., McCabe, E. R. B., Churchill, B. M., & Haake, D. A. (2007). *Journal of Molecular Diagnostics, 9*, 158–168.
26. Ulianas, A., Heng, L. Y., Lau, H. Y., Ishak, Z., & Ling, T. L. (2014). *Analytical Methods, 6*, 6369–6374.
27. Siddiquee, S., Yusof, N. A., Salleh, A. B., Bakar, F. A., & Heng, L. Y. (2010). *Bioelectrochemistry, 79*, 31–36.